Computational and Structural Biotechnology Journal 21 (2023) 472–484

Contents lists available at ScienceDirect

Computational and Structural Biotechnology Journal

journal homepage: www.elsevier.com/locate/csbj

TRRAP-mediated acetylation on Sp1 regulates adult neurogenesis

Bo-Kun Yin [a], David Lázaro [a], Zhao-Qi Wang [a,b,*]

[a] Leibniz Institute on Aging – Fritz Lipmann Institute (FLI), Beutenbergstrasse 11, 07745 Jena, Germany
[b] Faculty of Biological Sciences, Friedrich-Schiller-University of Jena, Bachstrasse 18k, 07743 Jena, Germany

ARTICLE INFO

Article history:
Received 25 October 2022
Received in revised form 15 December 2022
Accepted 15 December 2022
Available online 19 December 2022

Keywords:
TRRAP
HAT
SP1
Lysine acetylation
Adult neural stem cells

ABSTRACT

The adult hippocampal neurogenesis plays a vital role in the function of the central nervous system (CNS), including memory consolidation, cognitive flexibility, emotional function, and social behavior. The deficiency of adult neural stem cells (aNSCs) in maintaining the quiescence and entering cell cycle, self-renewal and differentiation capacity is detrimental to the functional integrity of neurons and cognition of the adult brain. Histone acetyltransferase (HAT) and histone deacetylase (HDAC) have been shown to modulate brain functionality and are important for embryonic neurogenesis via regulation of gene transcription. We showed previously that Trrap, an adapter for several HAT complexes, is required for Sp1 transcriptional control of the microtubule dynamics in neuronal cells. Here, we find that Trrap deletion compromises self-renewal and differentiation of aNSCs in mice and in cultures. We find that the acetylation status of lysine residues K16, K19, K703 and K639 all fail to overcome Trrap-deficiency-incurred instability of Sp1, indicating a scaffold role of Trrap. Interestingly, the deacetylation of Sp1 at K639 and K703 greatly increases Sp1 binding to the promoter of target genes, which antagonizes Trrap binding, and thereby elevates Sp1 activity. However, only deacetylated K639 is refractory to Trrap deficiency and corrects the differentiation defects of Trrap-deleted aNSCs. We demonstrate that the acetylation pattern at K639 by HATs dictates the role of Sp1 in the regulation of adult neurogenesis.

© 2022 The Author(s). Published by Elsevier B.V. on behalf of Research Network of Computational and Structural Biotechnology. This is an open access article under the CC BY-NC-ND license (http://creativecommons.org/licenses/by-nc-nd/4.0/).

1. Introduction

Brain development is tightly controlled and coordinated by complex genetic and environmental processes, an aberration of which can lead to neurodevelopmental disorders [1]. The synchronized function among neuronal and glia cells orchestrates variable actions ranged from simple tasks to complicate activities [2]. Neurogenesis is a process of generating newborn neurons and glial cells from neural stem cells (NSCs). In the adult mammalian brain, neurogenesis occurs in restricted regions of the brain: the subgranular zone (SGZ) of the dentate gyrus (DG) in the hippocampus and, the subventricular zone (SVZ) of the lateral ventricles (in mice), which generates neurons migrating to the olfactory bulb, and hypothalamus (in both humans and mice) [3–5]. The hippocampus consists of the Cornu Ammonis fields (CA1, CA2 and CA3) and the DG [6] and is the main region of the brain responsible for memory and learning [7]. The adult neurogenesis in the SGZ is mainly derived from adult neural stem cells (aNSCs) that differentiate into excitatory DG neurons and integrate into the inner circuitry of the hippocampus, connecting mainly to the CA3 pyramidal neuros, mossy cells and hilar interneurons [8]. The adult hippocampal neurogenesis is considered to play a vital role in maintaining multiple functions of the central nervous system (CNS), including memory consolidation, cognitive flexibility, emotional function, and social behavior [9–11].

The activation of quiescent aNSCs and the proper self-renewal and differentiation capacity of aNSCs are important for the functional adult brain [12,13]. Several diseases, such as Intellectual Disability (ID) and Autism Spectrum Disorders (ASD), show impaired adult hippocampal neurogenesis [14–16]. The cytoarchitecture of the septal and striatal SVZ, as a region of neonatal neurogenesis, is often altered in ASD patients [17]. Human Fragile-X Syndrome (FXS) is the most common form of inherited ID and the most important genetic cue of ASD, which exhibits alterations of the hippocampal volume [18,19] and a compromised hippocampal function [20,21]. FXS mouse model studies showed abnormal hippocampal functions due to defects of proliferation and differentiation of aNSCs during adult neurogenesis [22–24]. Many mouse models of ASD or ID demonstrated their link with defective adult neurogenesis in the SVZ

Abbreviations: TRRAP, Transformation/transcription domain-associated protein; HAT, Histone acetyltransferase

* Corresponding author at: Leibniz Institute on Aging – Fritz Lipmann Institute (FLI), Beutenbergstrasse 11, 07745 Jena, Germany,.
E-mail address: Zhao-Qi.Wang@leibniz-fli.de (Z.-Q. Wang).

https://doi.org/10.1016/j.csbj.2022.12.024
2001-0370/© 2022 The Author(s). Published by Elsevier B.V. on behalf of Research Network of Computational and Structural Biotechnology. This is an open access article under the CC BY-NC-ND license (http://creativecommons.org/licenses/by-nc-nd/4.0/).

[25–27]. These clinical and laboratory studies highlight the impairment of adult neurogenesis as the etiology of ASD/ID.

Histone acetyltransferase (HAT) and histone deacetylase (HDAC) conducts protein acetylation, originally described for histones, but also for other proteins [28]. HATs and HDACs have been shown to modulate brain functionality, including memory formation and neuroprotection [29–31]. The disturbance of the acetylation profile has been related to multiple neuropathological diseases, for instance, Huntington's disease [32], Parkinson's disease [33] and Alzheimer's disease, among others [34]. TRRAP, abbreviated for Transformation/transcription domain-associated protein, is a member of phosphatidylinositol 3-kinase-related kinases (PIKK) family. As the only pseudokinase (lacking the critical motifs required for ATP binding and catalysis, thereby missing the kinase activity) in the family, TRRAP acts as a scaffold protein mediating histone acetylation and transcription activation [35]. TRRAP is an adapter for two major HAT families: the general control nonderepressible-related (GCN5) acetyltransferase (GNAT) HAT family (e.g., Gcn5 and PCAF) and MOZ, Ybf2/Sas3, Sas2, TIP60-related (MYST) HAT family (e.g., TIP60) [28,35]. TRRAP is required for HAT activity, for instance TIP60 and PCAF, and co-activates target gene transcription [36–38]. Through interacting with transcription factors, TRRAP facilitates HAT binding to promoter regions of target genes, leading to acetylation of histone. This action enables the relaxation of chromatin conformation and facilitates the transcription process [39,40]. Depending on the cell type examined, the function of TRRAP target genes covers a wide range of cellular processes, including stem cell self-renewal and differentiation, hematopoietic stem cell pool maintenance, cancer progression and lipid metabolism [41–43].

Since Trrap deletion leads to peri-implantation lethality in mice [44], TRRAP null mutation is believed to cause embryonic lethality in humans. Recent studies identified 83 TRRAP variants in humans [45–47]. 17 distinct TRRAP variants were identified in 24 patients with neurodevelopmental disorders and mostly with malformation of diverse organs, including the brain, heart, kidney, or urogenital tracks [46]. Intriguingly, nearly half of these patients exhibit ASD and/or ID symptoms with variable severity, yet, lacking obvious malformation of brain architecture [46]. Using mouse models, we previously showed that Trrap deletion causes premature differentiation of embryonic neuroprogenitors (NPCs) by disrupting their cell cycle progression during neocortical neurogenesis [43]. While dissecting Trrap function in post-mitotic neurons, we demonstrated that Trrap is not required for development of Purkinje cells in the cerebellum, but prevents their degeneration in adult life [48]. These studies demonstrate the involvement of Trrap in the maintenance of embryonic neurogenesis and post-mitotic neurons. Molecularly, Trrap recruits Sp1 to chromatin and facilitates the Sp1 binding to the promoters of microtubule-destabilizing phosphoproteins STMN3 and STMN4 (STMN3/4) to maintain proper microtubule dynamics in neurons [48]. This study suggests that Trrap and/or HAT is required for Sp1 transcriptional activity. Yet, how Trrap regulates Sp1 remains elusive.

Sp1 is a master transcription factor that regulates the expression of genes involved in many cellular processes [49]. Sp1 activity can be regulated by multiple pathways including post-translational modifications (PTMs), such as phosphorylation [50], acetylation [51], SUMOylation [52] and ubiquitination [53]. For instance, PKC and MAPK cascades [54] and MEK-1 [55] can phosphorylate Sp1 to execute the transcriptional processes. p300 acetylates the K703 residue to repress Sp1 transcriptional activity [56]. TIP60 acetylates Sp1 at K639 impairing its promoter binding on target genes, thereby repressing its activity [57]. SUMOylation at K16 leads to proteasomal degradation of Sp1 [52]. It is also known that both acetylation and ubiquitination can modify the same residue K19 on Sp1 [58], suggesting that acetylation may stabilize Sp1 through competing against ubiquitin-mediated proteasomal degradation [59]. Therefore, PTMs at these lysine residues may crosstalk and modulate the activity and stability of Sp1.

In this study, we investigated the possible role of Trrap-dependent acetylation or its scaffold function on Sp1's transactivation in respect to adult neurogenesis. We identified that deacetylation at K639 residue on Sp1 ensures the aNSC differentiation process and Trrap, via its role in modifying Sp1 activity, is required for proper cell proliferation and differentiation of aNSCs.

2. Material and method

2.1. Inducible Trrap-deletion in vivo and in vitro

Mice carrying the conditional (floxed, *Trrap*$^{f/f}$) allele [44] were crossed with mice carrying the transgene *Nestin*-CreER^{T2} [60] (*Trrap*$^{f/f}$; *Nestin*-CreER^{T2}) or CreER^{T2} [61] (*Trrap*$^{f/f}$;*Rosa26*-CreER). All experiments were conducted according to German animal welfare legislation, and the protocol was approved by Thüringen Landesamt für Verbraucherschutz (TLV) (03–042/16), Germany.

2.2. Truncation and mutagenesis of Sp1 constructs

Human Sp1 was cloned into the pFLAG-CMV-2 plasmid using *Hin*dIII and *Xba*I restriction enzyme. Sp1 sequence was subcloned originally from the pcDNA3.1-V5-His-Sp1 plasmid kindly provided by Professor Xiaozhong Peng (Pekin Union Medical College, Beijing, China). Construction of truncation mutants followed the Sp1 truncation from previous study [62]. Mutagenesis on Sp1 construct was performed following the instruction of the QuikChange II XL Site-Directed Mutagenesis Kit (Agilent Technologies, Santa Clara, United States).

2.3. Histology and immunofluorescence staining

Tissues for histology were fixed in 4 % paraformaldehyde (PFA), cryoprotected in 30 % sucrose and frozen in Richard-Allan™ Scientific Neg-50™ Frozen Section Medium (Thermo Fisher Scientific, Waltham, MA, USA). Sections with thickness of 5–20 μm were used for immunofluorescence staining. Following antibodies/reagent were used for immunofluorescence staining: Rabbit anti-GFAP (1:300, Agilent), rabbit anti-Ki67 (1:200, Thermo Fisher Scientific), goat Sox2 (1:200, Santa Cruz Biotechnology, Dallas, United States), goat anti-doublecortin (DCX) (1:200, Santa Cruz), mouse anti-GFP (1:200, Santa Cruz), donkey anti-rabbit Cy5 (1:200 – 1:400, Jackson ImmunoResearch, West Grove, United States), rabbit anti-goat IgG Cy3 (1:200 – 1:400, Sigma-Aldrich, St. Louis, USA), Donkey anti-mouse Cy2 (1:200 – 1:400, Jackson ImmunoResearch) and DAPI (1:3000–1:5000, Thermo Fisher Scientific).

2.4. Inducible Trrap-deletion in aNSCs in vivo and in vitro

The genotypes of Trrap and Cre in mice were determined by PCR on DNA extracted from tail tissue, as previously described [42]. To induce *Trrap* deletion in Trrap-aNSCΔ mice, Tamoxifen (100 μg/g) (TAM, Sigma-Aldrich) was injected peritoneally during 5 consecutive days. To knockout *Trrap* in vitro, adult stem cells (aNSC) were isolated as previously described [48] and aNSCs were treated with 1 μM 4-hydroxytamoxifen (4-OHT, Sigma-Aldrich) for 3 days to induce Trrap deletion, followed by additional 2 days incubation in fresh medium.

2.5. aNSC cell culture and transfection

aNSCs were cultured in aNSC culture medium consisting of Dulbecco's Modified Eagle Medium/Nutrient Mixture F-12 (DMEM/F-12, Thermo Fisher Scientific), 1 × B-27™ Supplements (B27,

Thermo Fisher Scientific), 1 × penicillin–streptomycin, 20 ng/ml Animal-Free Recombinant Human EGF (Peprotech, Rocky Hill, United States), and 20 ng/ml Recombinant Human FGF-basic (bFGF, Peprotech). Prior to aNSCs seeding, 24-well culture dishes were coated with 50 mg/ml Poly-L-Lysine, (PLL, Sigma-Aldrich) and 10 mg/ml Laminin (Sigma-Aldrich). 3 × 10^5 aNSCs treated with 4-OHT were plated each well in Neurobasal™ Medium (NEM, Thermo Fisher Scientific) supplemented with 1 x B27, 2 mM L-glutamine, 1 × N-2 Supplement (N2, Thermo Fisher Scientific), 1 × penicillin–streptomycin, 20 ng/ml EGF, and 20 ng/ml bFGF. On the next day, transfection was performed on monolayer aNSCs. The Sp1 reporter (−111 hTF m3, Addgene plasmid # 15450), exogenous FLAG-Sp1 and CMV-GFP was mixed with Lipofectamine™ 2000 Transfection Reagent (Lipo2000, Thermo Fisher Scientific) and transfected into aNSCs. 24 h later, aNSC cultures were then subjected to luciferase assay. For in vitro differentiation, aNSCs were transfected using Lipo2000 mixed with plasmids in NEM supplemented with 500 μM L-glutamine (0.27 μg plasmid + 0.5 μl Lipo2000 in 370 μl/well in 24-well plate). After 30 min incubation, the plasmid-Lipo2000 mix was replaced by the original differentiation medium with supplement.

2.6. MG-132 treatment on aNSC

aNSCs were treated with 4-OHT for 3 days, followed by treatment with 20 μM MG-132 resuspended in fresh aNSC medium. The cells were then subjected to immunoblotting analysis.

2.7. N2A cell culture and plasmid transfection

Neuroblastoma cell line N2A was cultured in Dulbecco's Modified Eagle Medium (DMEM, Thermo Fisher Scientific) supplemented with 1 × FCS, 1x penicillin-streptomycin, and 1 mM sodium pyruvate (Thermo Fisher Scientific). Cells were passaged every 2–3 days in 1:12 ratio when the N2A culture reached ~70 % confluency. For transfection, cells were seeded in 2.8 × 10^5 cells/well onto 6-well plate. The transfection of N2A cells was performed with polyethylenimine (PEI, Polyscience, Eppelheim, Germany) at a ratio of 1 μg plasmid per 3 μg PEI. 24 h after transfection, the cells were harvested for co-immunoprecipitation (co-IP), ChIP, or immunoblotting.

2.8. Trrap knockdown and transfection in N2A cells

siRNA against Trrap (Cat#: LQ-051873–01–0005, Horizon Discovery, Waterbeach, United Kingdom) was mixed with Lipofectamine™ RNAiMAX Transfection Reagent (Thermo Fisher Scientific) and transfected into N2A cells. After 24 h transfection, Sp1 construct was then mixed with PEI and transfected into N2A. N2A cells were then incubated for another 24 h and subjected to co-IP analysis.

2.9. Proliferation assay by IncuCyte

The aNSC culture was seeded 5 × 10^4 per well in 50 ml/ml PLL- and 10 mg/ml Laminin-coated 24-well plate and incubated in IncuCyte S3 (Sartorius AG, Göttingen, Germany) for imaging acquisition of phase contrast (10× magnification, 36 images/well in 24-well plate). The confluency of aNSCs and video recording of cells proliferation was determined through Incucyte® Live-Cell Analysis.

2.10. In vitro aNSC differentiation

2–4 × 10^4 aNSCs were resuspended with aNSC plating medium (DMEM/F-12 medium supplemented with 1× N2 (Thermo Fisher Scientific) and 20 ng/ml bFGF and plated onto 50 μg/ml Poly-L-Orthinine- (PLO, Sigma-Aldrich) and 10 μg/ml laminin-coated 12 mm glass coverslips. After 24 h, the medium was replaced by the aNSC differentiation medium (DMEM/F-12 with 1 × B27 Supplements, 1 × N2 Supplement, 2 mM L-glutamine, 0.5 % FBS, 20 ng/ml bFGF and 0.5 μM retinoic acid). Half of the medium was refreshed once every 2 days. The aNSCs were processed for immunostaining at 1-, 4-, 5- or 9-day post-differentiation (DPD). The aNSC transfection during in vitro differentiation was performed at 2 DPD.

2.11. Immunofluorescent staining and quantification

aNSCs were fixed with 4 % PFA and permeabilized with 0.7 % Triton diluted in DPBS, no calcium, no magnesium (PBS, Thermo Fisher Scientific) for 15 min. Samples were then incubated with primary antibodies (resuspended in PBS supplemented with 1 % BSA, 5 % donkey serum and 0.1 % Triton) under 4 °C overnight. After being washed with PBS, the samples were then further incubated with secondary antibodies (resuspended in PBS supplemented with 7 % BSA and 1:1000 DAPI) for 1 h. The samples were then conserved by ProLong™ Gold Antifade reagent (Thermo Fisher Scientific). Following antibody/reagent were used for immunofluorescence staining: mouse anti-Tubulin βIII (Tuj1, 1:400, Covance, Princeton, United States), sheep anti-mouse IgG Cy3 (1:400, Sigma-Aldrich) and DAPI (1:3000). The coverslips were then imaged by the ZEISS Apotome 3 (Carl Zeiss AG, Jena, Germany) under the 20x or 40x objectives. The neuron population was then scored with ImageJ software and numerated manually.

2.12. Luciferase assay

24 h after transfection, aNSCs were then lysed and cell lysates were subjected to activity assay according to the instruction by Dual-Glo® Luciferase Assay System (Promega, Madison, United States). The luciferase activity was then normalized by the total cell protein concentration measured with the Pierce™ BCA Protein Assay Kit (BCA assay, Thermo Fisher Scientific).

2.13. Immunoblot analysis

Total protein lysates were prepared from aNSCs with the RIPA buffer (50 mM Tris- HCl, pH 7.4, 150 mM NaCl, 1 % NP40, 0.25 % Na-deoxycholate, 1 mM EDTA, 1 mM PMSF), and cOmplete™ Protease inhibitor-Cocktail (protease inhibitor, Roche, Basal, Switzerland). Protein was quantified using the BCA Assay. Immunoblotting was performed as described previously [48], using the following antibodies: mouse anti-TRRAP (1;1000, Euromedex, Souffelweyersheim, France), mouse anti-Cdc25A (1:500, Santa Cruz), rabbit anti-Cyclin D1 (1:500, Santa Cruz), mouse anti-Mad2 (1:1000, BD Biosciences, Franklin Lakes, United States), mouse anti-FLAG (1:1000, Sigma-Aldrich), rabbit anti-Sp1 (1:1000, Merck Millipore, Burlington, United States), mouse anti-b-actin (1:5000, Sigma-Aldrich), mouse anti-GFP (1:400, Santa Cruz) and rabbit anti-Plk1 (1:1000, Abcam, Cambridge, United Kingdom).

2.14. Co-IP

For co-IP, cells were harvested with NET-N buffer (50 mM Tris–HCl (pH 7.5), 150 mM NaCl, 5 mM EDTA, 0.5 % NP-40, and protease inhibitor. Approximate 1 mg of total lysate was incubated with the Dynabeads™ Protein A Immunoprecipitation Kit (Thermo Fisher Scientific) and 2 ug mouse anti-FLAG antibodies at 4 °C overnight. The precipitates were then washed with the NET-N buffer with protease inhibitor, followed by elution with SDS buffer lysis

buffer (50 mM HEPES-KOH, 140 mM NaCl, 1 mM EDTA, 0.1 % Triton X-100, 0.1 % sodium deoxycholate, 1 % SDS, 10 mM NaB, and protease inhibitor) and immunoblot analysis. Immunoblotting was performed using the following antibodies: mouse anti-TRRAP (1;1000, Euromedex, Souffelweyersheim, France), mouse anti-FLAG (1:1000, Sigma-Aldrich), mouse anti-β-actin (1:5000), goat anti-TIP60 (1:500 Santa Cruz), goat anti-mouse HRP (1:3000, Agilent), goat anti-rabbit HRP (1:3000, Agilent) and rabbit anti-goat HRP (1:3000, Agilent).

2.15. Chromatin immunoprecipitation (ChIP) assay

Transfected N2A cells were wash with PBS and collected with cell scraper, followed by the same protocol as previously described [48].

2.16. Statistical analysis

The statistical analysis was performed through GraphPad (Dotmatics, Boston, United States). Paired/unpaired t-test or Two-Way ANOVA were performed on the respective data labeled in the figure legends.

3. Results

3.1. Deletion of Trrap abrogates adult neurogenesis

To study the role of Trrap-HAT in aNSCs, we first generated TAM-inducible and traceable deletion of *Trrap* in mice. For this, *Trrap*$^{f/f}$ mice [44] were crossed with mice carrying the transgene *Nestin*-CreER^{T2} [60] to produce *Trrap*$^{f/f}$;*Nestin*-CreER^{T2} mice, which upon TAM treatment generates inducible Trrap deletion in neural stem cells in adult mice (designated Trrap-aNSCΔ). To trace Trrap-deleted cells in vivo, Trrap-aNSCΔ mice were subsequently crossed with double-fluorescent reporter *mT/mG* knock-in mice [63]. This reporter allows monitoring of Trrap-deleted cells by GFP expression, after switching from Tomato by Cre recombination in the aNSCs in the DG and SVZ. *Trrap*$^{f/+}$ mice with the Cre transgene showed no detectable abnormalities and were used as controls.

We analyzed mutant mice at 1- and 5-months post-TAM injection (MPT). Co-immunostaining of brain sections revealed that Trrap deletion yielded a great decrease in aNSC proliferation (judged by GFP$^+$Ki67$^+$) and an increase of cell death (GFP$^+$TUNEL$^+$), as early as 1 MPT (Fig. 1A-C). Co-staining of GFP with the aNSC markers GFAP and Sox2 in Trrap-aNSCΔ brain detected a progressive decrease of the aNSC pool (GFAP$^+$Sox2$^+$ with the radial glia morphology characteristic of the aNSCs localized in the SGZ of the DG) during 1–5 MPT (Fig. 1D-E). Intriguingly, we found a great increase of GFAP$^+$Sox2$^+$ cells localized outside the SGZ of the DG, characterized by a protoplasmic-spongiform morphology (Fig. 1D, F), indicative of astrocytes. In addition, co-staining of GFP together with a newborn neuron marker DCX, showed a great reduction of newborn neurons (GFP$^+$DCX$^+$) at 1 MPT and a complete absence of newborn neurons at 5 MPT (Fig. 1G-H). These results indicate that Trrap deletion results in a progressive loss of the self-renewal capacity of aNSCs. The decline of neuronal differentiation correlates with greatly increased astrocytes, suggesting a differentiation defects of Trrap-deleted aNSCs.

3.2. Trrap deletion compromises proliferation and differentiation of aNSCs in vitro

To further investigate the cell autonomous function of Trrap in the proliferation and differentiation of aNSCs, we generated a mouse line *Trrap*$^{f/f}$;*Rosa26*-CreER (*Trrap*$^{f/f}$-CreER) [48] by crossing *Trrap*$^{f/f}$ mice with *Rosa26*-CreER mice [61] and isolated aNSCs from these mice at the age of 2–3 months. Incubation of aNSCs, derived from *Trrap*$^{f/f}$; *Rosa26*-CreER mice, with 4-OHT resulted in efficient deletion of the *Trrap* allele (designated TrrapΔ-aNSC) as confirmed by PCR genotyping (Fig S1A). Trrap$^{f/+}$-CreER aNSCs with 4-OHT treatment (Fig S1B) were used as control as previously described [48].

To monitor the proliferation, we used the IncuCyte assay following and measuring in live the confluency of aNSC monolayer culture (Fig. 2A). We found a great delay of the confluency of mutants than controls, indicative of a lower proliferation rate (Fig. 2A-B, Video S1–2). Next, we analyzed the differentiation capacity of aNSCs using a modified in vitro differentiation protocol [64] (Fig S1C). The identity of the cell mixture was monitored by immunostaining with the neuronal marker Tuj1 at different DPD. The neuron population (Tuj1$^+$) in control aNSCs was increased at 1 DPD and reached about 15 % in the culture between 4 and 5 DPD, which then remained stable until 9 DPD (Fig. 2C-D). In contrast, Trrap-deleted aNSCs gave rise to only a significantly lower number of neurons compared to control (Fig. 2C-D). The mutant neuron population occupied less than 10 % of the cultures at 4–5 DPD, followed by a drop to 4 % at 9 DPD (Fig. 2C-D). These findings indicate that the differentiation capacity of Trrap-deficient aNSCs is lost much faster compared to that of control cells. Thus, Trrap is required for proper proliferation and differentiation of aNSCs.

Supplementary material related to this article can be found online at doi:10.1016/j.csbj.2022.12.024.

3.3. Sp1 interacts with Trrap

We showed previously that Trrap facilitates Sp1 binding to promoters to initiate transcription of its target genes STMN3/4 [48]. Sp1 has been shown to interact with diverse coactivators to enhance its transcriptional activity [49]. We questioned if the presence of Trrap itself is necessary for the Sp1 activity. To this end, we performed an interaction study between Sp1 and Trrap. We constructed various truncation mutants of Sp1 based on the previously defined transcription activation domains [62] (Fig. 3A). Co-IP in neuroblastoma N2A cell line after transfection of indicated mutant Sp1 vectors revealed various interaction strength between Sp1 and endogenous Trrap, but with a strong interaction via the transactivation domains A and B (Fig. 3A-B), which have been shown to facilitates Sp1 transcription activity [65].

3.4. Sp1 stability in Trrap mutant cells is not affected by the acetylation status of K16 and K19 on Sp1

Previously, we found that Sp1 activity was greatly reduced in Trrap deficient cells while the Sp1 mRNA level was unaltered in these cells [48]. To further study whether Sp1 activity was affected by protein expression, we performed Western blotting and detected a very low Sp1 level in TrrapΔ-aNSC cells compared to controls (Fig. 4A), which however could be greatly improved by proteasome inhibitor MG-132, indicating that the decrease of Sp1 is due to proteasome degradation (Fig. 4A). K16 and K19 residues have been hinted for Sp1 stability. It is assumed that acetylation of these residues, potentially competes against the SUMOylation [52] and ubiquitination processes [58], thus interfering the stabilization of Sp1 [59]. Therefore, we reasoned that Trrap-deletion impairs acetylation thereby facilitating ubiquitination and SUMOylation of these lysines, which might render Sp1 undergoing proteasomal degradation.

To further understand how Sp1 stability is affected by Trrap, we next analyzed lysine acetylation of Sp1. To this end, we constructed

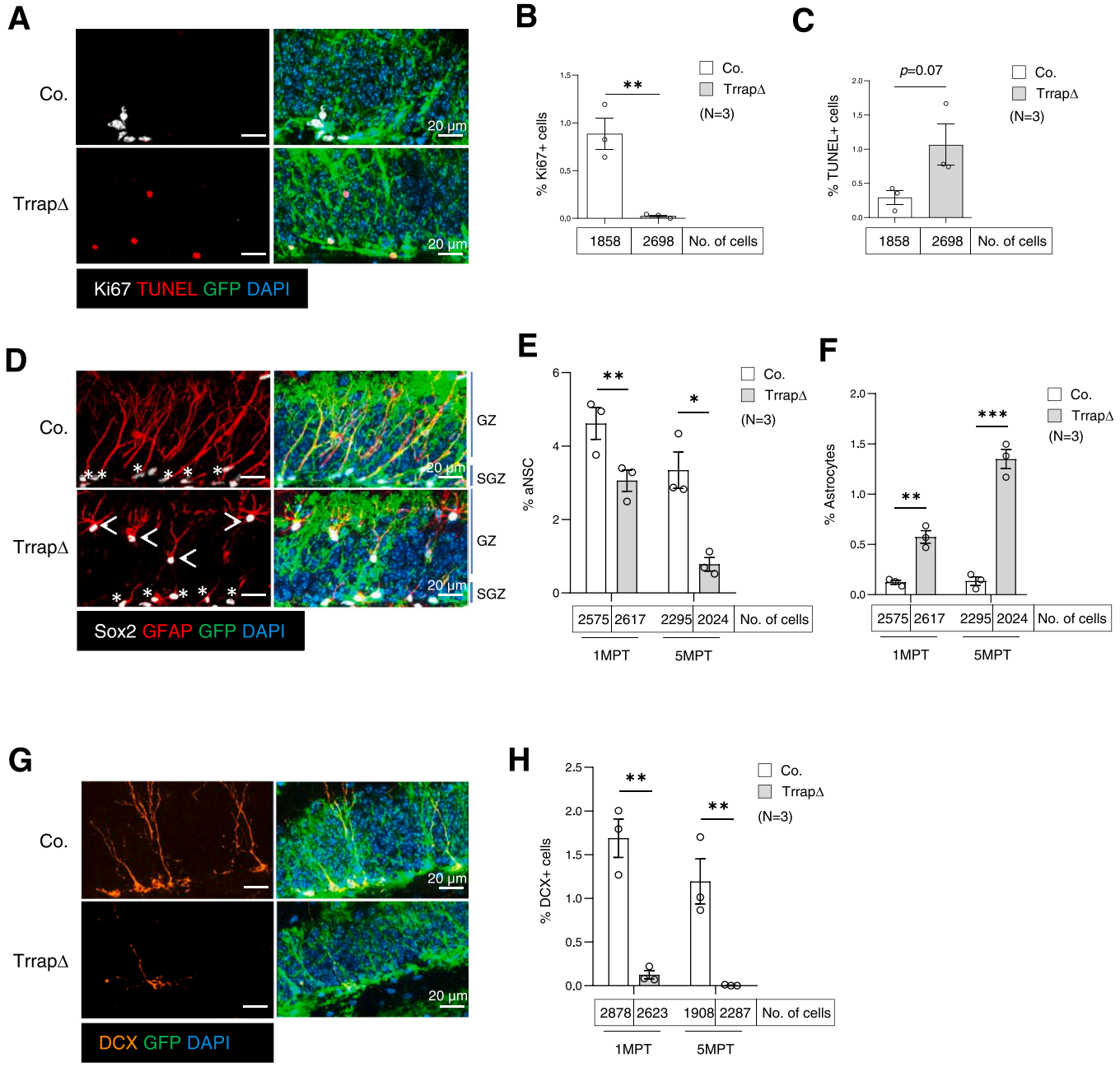

Fig. 1. Deletion of Trrap in aNSCs abolishes the adult neurogenesis. A. Representative images of DG sections from 1 MPT. DG sections were stained with antibodies against Ki67 (white, proliferative cells) and GFP (green, recombinant *Trrap* knockout cells), and co-stained with the reagent of TUNEL reaction (red, cell death) and DAPI (cyan). B-C. The quantification of the proliferative (Ki67$^+$) and apoptotic (TUNEL$^+$) cells in the DG of control and Trrap-aNSCsΔ mice at 1 MPT. Lower panel indicates the scored cell amount in total. 3 Trrap$^{f/+}$ and 3 Trrap-aNSCΔ mice analyzed. D. Representative images of DG sections from 5 MPT. DG sections were stained with antibodies against Sox2 (white, stem cell marker), GFAP (red, stem cell marker), GFP (green, recombinant *Trrap* knockout cells) and counterstained with DAPI (cyan). The aNSCs were identified by their soma located in the subgranular cell layer (asterisk) and the newborn astrocytes by their somas located in the granular cell layer (arrowhead). E-F. The quantification of aNSCs (Sox2$^+$GFP$^+$) and newborn astrocytes (GFAP$^+$GFP$^+$) in the DG at the indicated MPT. Lower panel indicates the scored cell amount in total. 3 Trrap$^{f/+}$ and 3 Trrap-aNSCΔ mice analyzed. G. Representative images of DG sections from 5 MPT stained with antibodies against DCX (orange), GFP (green, recombinant *Trrap* knockout cells) and co-stained with DAPI (cyan). H. The quantification of newborn neurons (DCX$^+$GFP$^+$) in the DG at the indicated MPT. 3 Trrap$^{f/+}$ and 3 Trrap-aNSCΔ mice analyzed. Co.: Trrap$^{f/+}$-aNSC; Δ: Trrap-aNSCΔ. Scale bar: 20 μm. Mean ± standard error of mean is shown. Unpaired t-test was performed for statistical analysis in (B-C), (E-F) and (H). *: $p \le 0.05$, **: $p \le 0.01$, ***: $p \le 0.001$.

Sp1 mutants by replacing both K16 and K19 with either an acetylation-incompetent residue arginine (R) (Sp1-K16R/K19R) or an acetylation-mimicking residue glutamine (Q) (Sp1-K16Q/K19Q). We transfected the FLAG-tagged respective Sp1 vectors together with a GFP vector (which monitors transfection efficiency) into aNSCs. We detected slightly lower, albeit non-significant, GFP levels in TrrapΔ-aNSCs compared to control cells. Strikingly, all Sp1 vectors (judged by FLAG), regardless of wildtype or mutant, could not be expressed efficiently in Trrap mutant cells compared to control cells (Fig. 4B-C). Nevertheless, K16R/K19R mutant Sp1 expressed higher Sp1 in

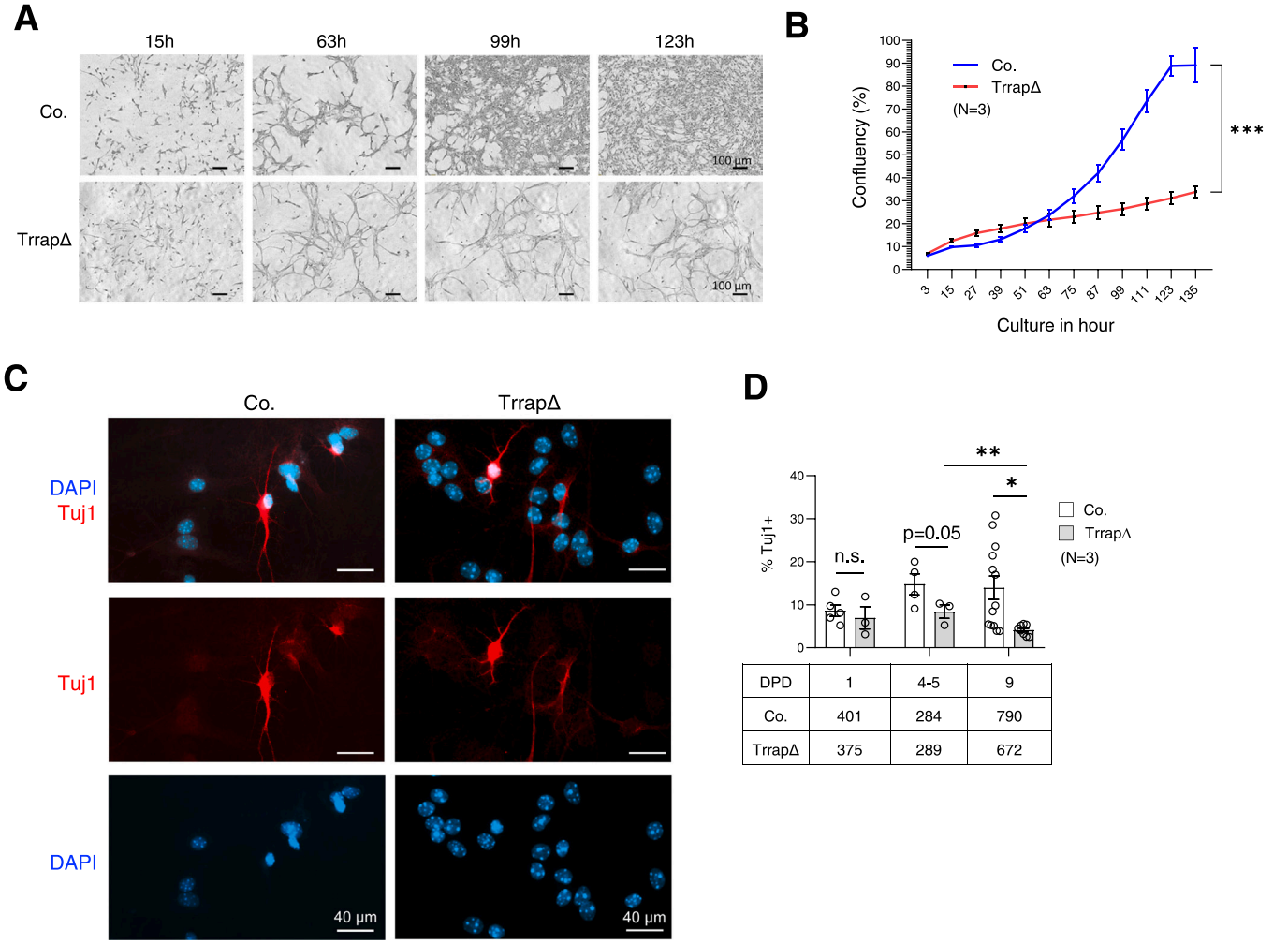

DPD	1	4-5	9
Co.	401	284	790
TrrapΔ	375	289	672

Fig. 2. Deletion of Trrap reduces the differentiation potential and proliferative rate in aNSCs, A. Live-cell monitoring by IncuCyte® determining the confluency of monolayer aNSC at the indicated incubation time. Images were taken under phase contrast and the 10× objective. Scale bar: 100 µm. B. Cell confluency of control and TrrapΔ-aNSCs over time monitored by Incucyte® Live-Cell Analysis. Cells originated from 3 mice analyzed. C. Immunofluorescent images showing the differentiation states of aNSCs at 9 DPD. Cell mixture was stained against neuronal marker Tuj1 (red) and co-stained with DAPI (cyan). D. Quantification of Tuj1^{+} cells in percentage to total cell population (DAPI^{+}). Cells from 3 to 5 Trrap$^{f/+}$ and Trrap-aNSCΔ mice at each DPD were analyzed. Scale bar: 40 µm. Mean ± standard error of mean is shown. Unpaired t-test was performed for statistical analysis in (C). Two-way ANOVA was performed for statistical analysis in (B). n.s.: not significant. *: $p \leq 0.05$, **: $p \leq 0.01$, ***: $p \leq 0.001$.

comparison with the wildtype Sp1 construct after normalization of the Sp1 level with actin in control cells (Fig. 4B-C). Sp1-K16Q/K19Q also showed slightly higher, albeit non-significant, Sp1 protein levels than wildtype Sp1 (Fig. 4B-C). However, both Sp1-K16R/K19R and Sp1-K16Q/K19Q mutants did not elevated significantly Sp1 compared to wildtype Sp1 in TrrapΔ-aNSCs (Fig. 4B-C), suggesting that although both lysine residues have conferred a stability to Sp1, their stability is still severely compromised in the Trrap mutant background.

Next, we analyzed the activity of ectopically expressed Sp1 proteins (Fig. 4D) after normalization with the exogenous Sp1 level judged by FLAG. We co-transfected Sp1 constructs with Sp1 reporter into aNSCs and performed luciferase assay as previously described [48]. All Sp1 constructs expressed significantly lower activity in TrrapΔ-aNSCs (Fig. 4D). Interestingly, Sp1-K16R/K19R increased the Sp1 activity in control cells but not in mutant cells. Given that the activity and protein levels of Sp1-K16R/K19R and -K16Q/K19Q are lower in the mutant, Trrap does not influence the acetylation status on K16 and K19. However, the deacetylation mutation at of K16 and K19 increased the Sp1 activity in control cells, strongly suggesting that apart from affecting Sp1 stability, these residues might also contribute to the regulation of Sp1 activity. Taken altogether, both residues do not seem to be involved in acetylation-related Sp1 stabilization, which nevertheless depends on the presence of Trrap to activate Sp1 in an unknown mechanism.

3.5. Acetylation of K639, but not K703, affects Trrap-dependent Sp1 activity

Sp1 can be acetylated at the K703 residue and the deacetylation of K703 increases Sp1 activity [56]. Next, we transfected FLAG-tagged wildtype Sp1 (FLAG-Sp1-WT) and two K703 mutant constructs (FLAG-Sp1-K703Q, FLAG-Sp1-K703R) together with GFP into aNSCs and analyzed their stability and activity. Western blotting revealed no obvious differences of expression between mutant and wildtype Sp1 vectors (Fig. 5A). However, all these vectors expressed significantly lower in Trrap mutant cells compared to control cells (Fig. 5A-B). Analog to previous findings [56], acetylation incompetent Sp1-K703R had a higher activity compared to Sp1-WT and also to Sp1-K703Q in

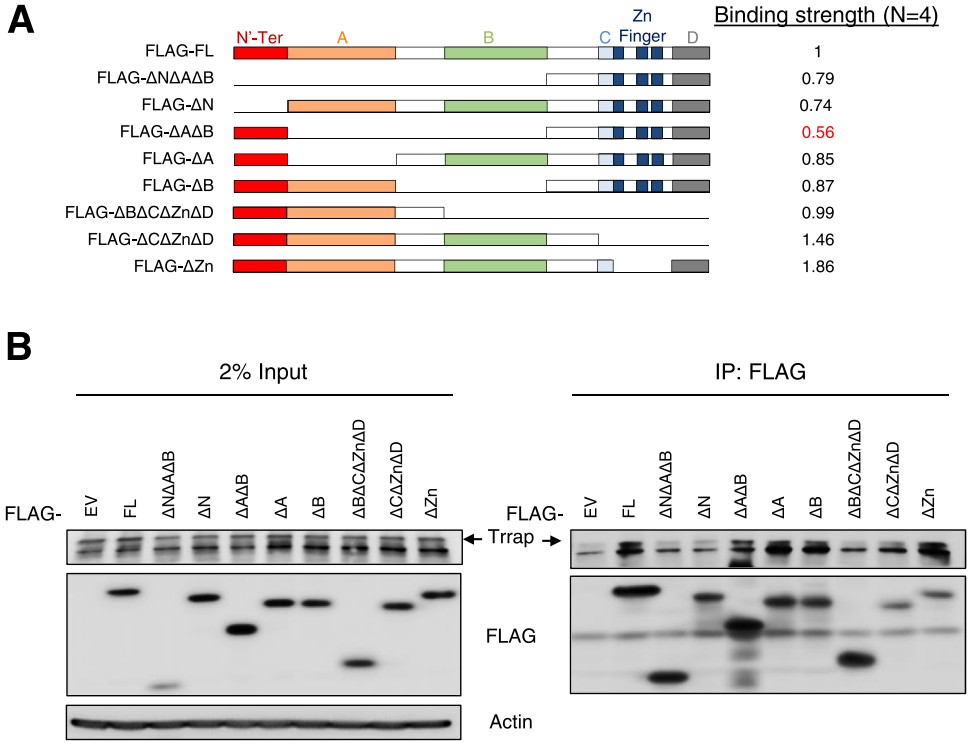

Fig. 3. Trrap interacts with Sp1 through the A, B domains, A. Sp1 truncation mutant constructs for Sp1-Trrap interaction assay. All truncations contain FLAG-tag at the N-terminus. Colored domains represent characterized ones on Sp1, while white regions are undefined. On the right side of each construct, the interaction strength between Sp1 truncation and Trrap (see panel (B)) is shown. N = 4. B. Co-IP result shows the interaction between each Sp1 truncation and endogenous Trrap in N2A cells. Cells were transfected with the indicated constructs and subjected to co-IP. Pulled-down samples were then analyzed by immunoblotting. Left panel shows the input level of transfected constructs. Actin blot acts as a loading control. On the right panel, the pulled-down samples were blotted by FLAG (indicating Sp1) and Trrap antibodies. The interaction strength (panel (A)) is determined by quantifying Trrap band (The upper band in Trrap blot) with the intensity of the FLAG band.

wildtype cells (Fig. 5C). Of note, the K703R mutant elevated the Sp1 activity in mutant cells to the level of Sp1-WT transfected wildtype cells (Fig. 5C), indicative of rescuing Sp1 activity defect incurred by Trrap knockout. Sp1-K703R had a 4.6-fold higher Sp1 transcriptional activity in control cells compared to mutant cells. However, the ratio of exogenous Sp1 activity between control and mutant cells was similar in Sp1-WT- and Sp1-K703R-transfected cells (3.5 folds vs 2.8 folds) (Fig. 5C). In contrast, the acetylation mimic Sp1-K703Q reduced Sp1 activity in both wildtype and Trrap mutant aNSC cells (Fig. 5C). In TrrapΔ-aNSCs, K703Q had even much lower activity compared to that in control cells, suggesting that acetylation at K703 indeed represses Sp1 activity, but likely independent of the Trrap scaffold function on HAT.

Next, we investigated another acetylated residue K639, which can be acetylated by the Trrap interacting partner TIP60 [57]. Co-IP experiments revealed an interaction between Sp1 and TIP60 in N2A cells, which however was abolished by Trrap knockdown (Fig. 6A), indicating that Trrap bridges both Sp1 and TIP60. To examine whether Trrap-TIP60 mediates acetylation of K639 on Sp1, we transfected Sp1-WT and acetylation-incompetent mutant Sp1 vectors (Sp1-K639R) into mutant and control aNSCs. Western blot analysis detected a lower expression of Sp1-WT and Sp1-K639R in Trrap mutant cells than that in control cells (Fig. 6B), demonstrating that K639 deacetylation does not reverse Sp1 destabilization incurred by Trrap-deletion. Strikingly, overexpressed K639R increased Sp1 activity to a similarly high level in both mutant aNSCs and controls (Fig. 6C). The activity of exogenous Sp1-K639R in mutant cells, after normalization with the FLAG level (i.e., amount of exogenous Sp1), was even comparable, if not more, than control (Fig. 6D), indicating that K639R overrides Trrap deficiency-incurred low Sp1 activity. This result lets us conclude that Trrap mediates the acetylation status on K639 on Sp1.

3.6. Chromatin binding of K639 and K703 mutant Sp1 at target gene promoters

We further explored how deacetylation mutant Sp1-K703R and Sp1-K639R increased Sp1 activity. To this end, we transfected Sp1-WT and mutant vectors into N2A cells and performed chromatin immunoprecipitation (ChIP) assay to examine their binding onto promoters of two Sp1 targets, p21 [66] and STMN3 [48]. We found that both K639R and K703R increased Sp1 binding on these promoters correlating well with their increased activity (Fig. 7A). Although K703Q abolished Sp1 activity, the promoter-binding is not affected (Fig. 7A). Intriguingly, Co-IP analysis revealed that Sp1-K639R or Sp1-K703R had lower Sp1-Trrap interaction, while acetylation mimic Sp1-K703Q did not significantly reduce this interaction, compared to Sp1-WT (Fig. 7B). Taken together, these results suggest that Sp1 deacetylation at these two lysine residues facilitates its chromatin binding but prevents its interaction with Trrap.

3.7. Deacetylation at K639 of Sp1 is required for aNSC differentiation

K639 is a key site that regulates Sp1 activity under Trrap-TIP60-mediated acetylation (Fig. 7A-B). To study the biological meaning of Sp1 deacetylation at K639, we transfected FLAG-Sp1-K639R and FLAG-EV into aNSCs and examined the differentiation of these cells. Ectopic expression of Sp1-K639R increased the neuron population in TrrapΔ-aNSCs at 5 DPD compared to cells transfected with FLAG-EV

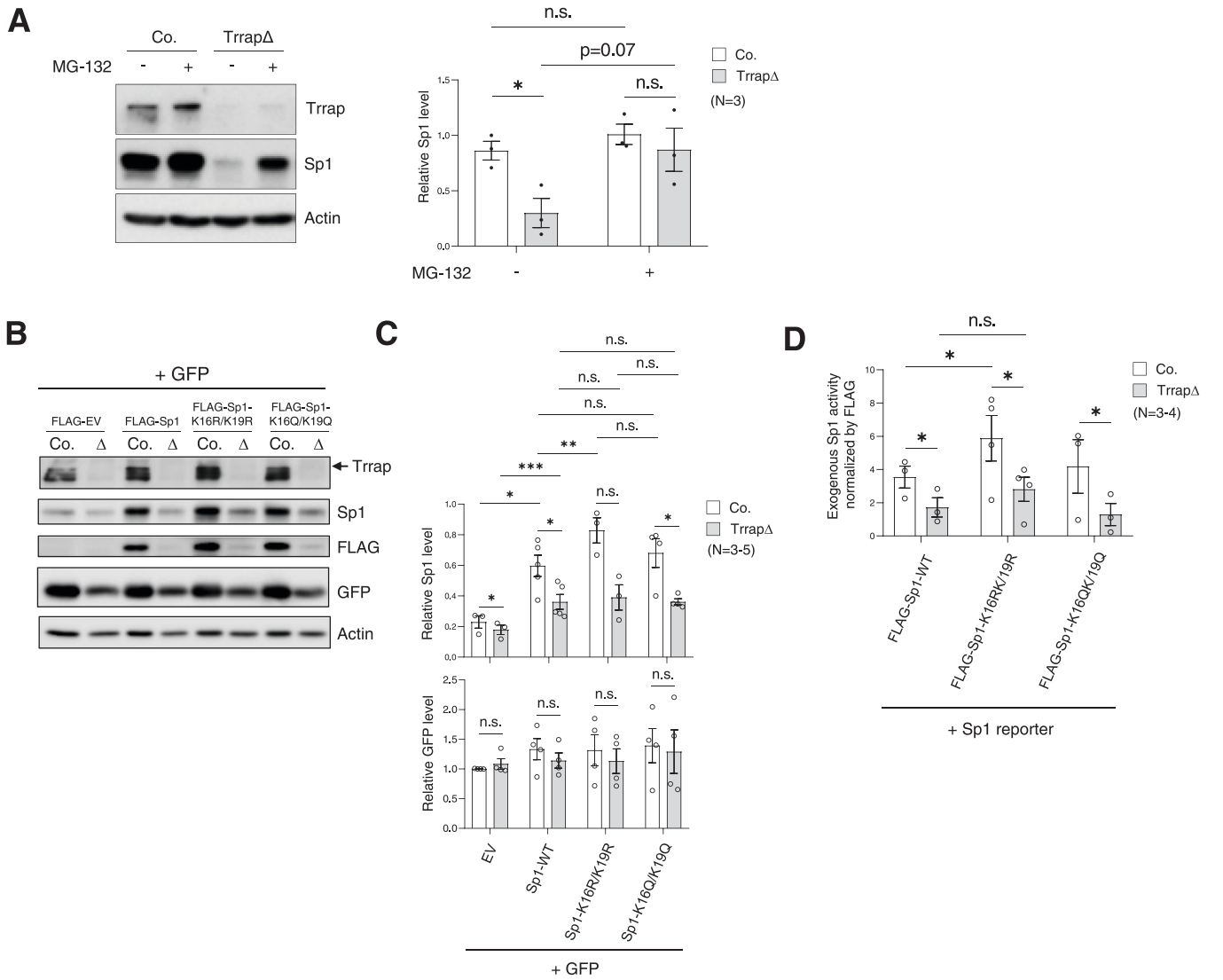

Fig. 4. Trrap stabilize Sp1 without affecting the K16 and K19 residue, A. Immunoblot showing the Sp1 level in Trrap$^{f/+}$-aNSCs and TrrapΔ-aNSCs with or without proteasomal inhibitor MG-132. aNSCs were treated with 4-OHT for 3 days and subjected to MG-132 treatment for 6 hr followed by immunoblot analysis using the indicated antibodies. Actin serves a loading control. Right panel shows the quantification of the immunoblots. Cells from 3 Trrap$^{f/+}$ and Trrap-aNSCΔ mice were analyzed. B. Immunoblot showing the level of exogenous Sp1 variants and the total Sp1 in both control and mutant aNSCs co-transfected with FLAG-Sp1-WT, FLAG-Sp1-K16R/K19R or FLAG-Sp1-K16Q/K19Q variants and GFP. C. The quantification of respective Sp1 and GFP level of (B). Cells from 3 to 5 Trrap$^{f/+}$ and Trrap-aNSCΔ mice analyzed. D. The activity of exogenous Sp1 variants was calculated by the exogenous Sp1 activity (subtracting the endogenous Sp1 activity from the whole Sp1 activity) divided by the exogenous Sp1 level (FLAG). The total Sp1 activity from control and mutant aNSC transfected with the indicated constructs together with Sp1-reporter based on the total cell protein concentration measured by the BCA assay (see Materials and Methods). Cells from 3 to 4 Trrap$^{f/+}$ and Trrap-aNSCΔ mice analyzed. Mean ± standard error of mean is shown. Unpaired t-test was performed for statistical analysis in (A) and paired t-test was performed for statistical analysis in (C-D). n.s.: not significant. *: $p \le 0.05$, **: $p \le 0.01$, ***: $p \le 0.001$.

(Fig. 7C-D), indicating that the differentiation of aNSCs is indeed controlled by the K639 deacetylation on Sp1 via Trrap-mediated HATs.

4. Discussion

A wealth of evidence indicates the involvement of the HAT and HDAC complexes in brain development and the maintenance of adult neurogenesis in the brain [29,67,68]. We previously showed in mouse models that Trrap is essential for embryonic neurogenesis by controlling cell cycle progression [43] and that Trrap maintains homeostasis of post-mitotic neurons by modulating the microtubule dynamics through transcription factor Sp1 [48]. In the current study, we find that Trrap-deficiency impairs the quiescence, expansion and differentiation capacity of aNSCs in vivo and in vitro. We identify that the forced deacetylation at K639 of Sp1, which disrupts its binding with Trrap, increases Sp1 binding to chromatin and its transcriptional activity. Ectopic expression of this mutant Sp1 reverses the differentiation defect of Trrap-deleted aNSCs. These data unravel a novel function of Trrap-HAT in adult neurogenesis via modulation of Sp1 acetylation.

Consistent with the in vivo mouse model, Trrap deletion in cultured aNSCs also compromised their proliferation and neuron formation, indicating that the effect of Trrap deletion is cell-autonomous. Notably, the mutant neuronal population decreased progressively from 5 DPD to 9 DPD, which corroborates the progressive loss of neuronal population in Trrap-aNSCΔ mouse model in vivo, possibly due to the loss of neuronal maintenance [48] and

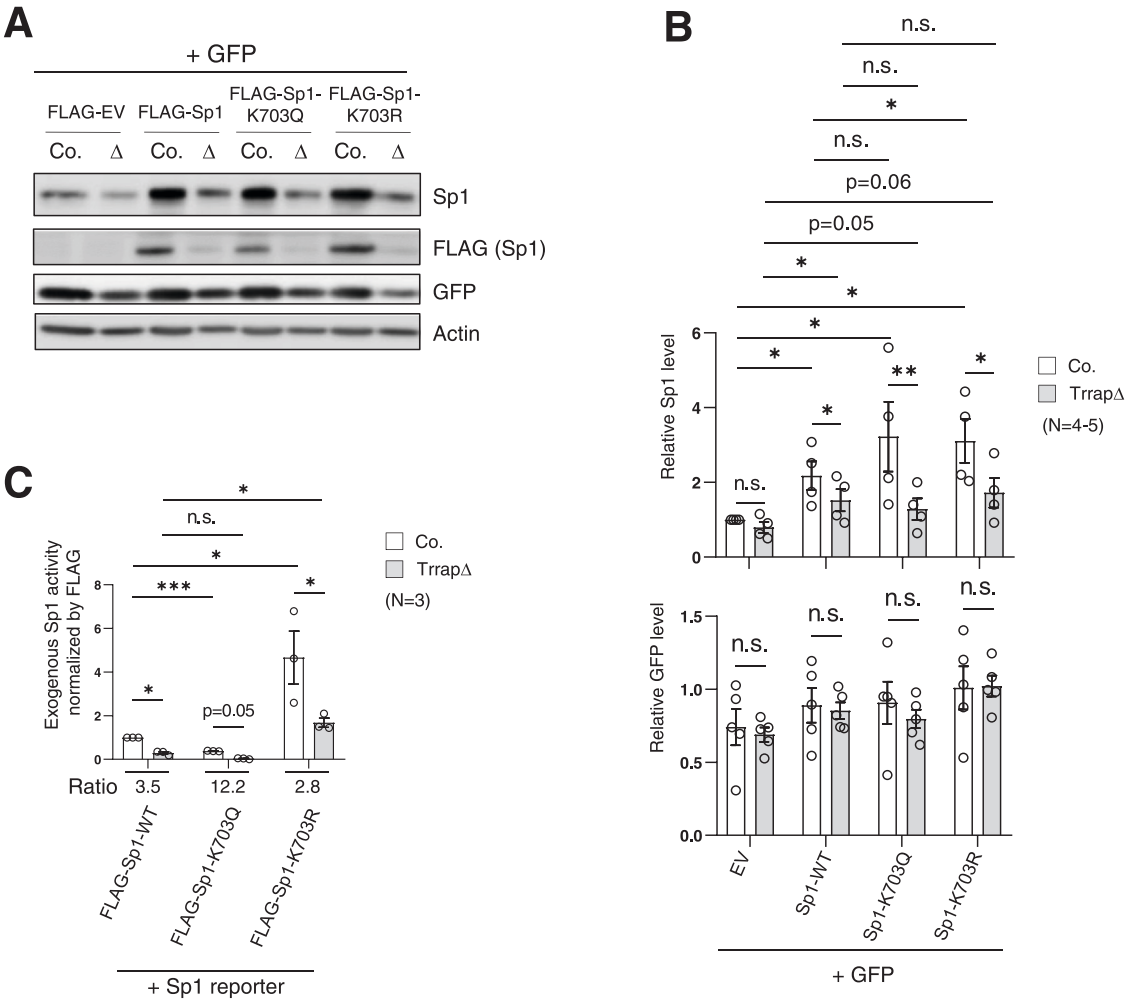

Fig. 5. Trrap does not affect the Sp1 activity through K703 acetylation,. A. Immunoblot shows the exogenous level of Sp1 variants (by FLAG) and whole Sp1 level in both control and mutant aNSCs co-transfected with FLAG-Sp1, FLAG-Sp1-K703Q or FLAG-Sp1-K703R variants together with GFP. Actin serves a loading control. B. The quantification of whole Sp1 level and GFP level is shown. Cells from 4 to 5 Trrap$^{f/+}$ and Trrap-aNSCΔ mice analyzed. C. The total Sp1 activity and the activity of exogenous Sp1 variants was calculated as described in Fig. 4D. Cells from 3 Trrap$^{f/+}$ and Trrap-aNSCΔ mice analyzed. Mean ± standard error of mean is shown. Paired t-test was performed for statistical analysis in (B), (C). n.s.: not significant. *: $p \leq 0.05$, **: $p \leq 0.01$, ***: $p \leq 0.001$.

also the exhaustion of the neuroprogenitor pool [43]. Interestingly, we noticed a reverse correlation of the neuron production with a great increase of astrocytes in vivo, indicating a disturbed differentiation program in aNSCs without Trrap. The conversion from the neurogenic to astrocytic differentiation of aNSCs is reminiscent of a process described for aNSC aging and aging-related depletion of the adult neurogenesis [69]. Nevertheless, we cannot completely rule out the possibility that increased astrocytes could be due to “stress” signals, imposed by Trrap deletion. We conclude that Trrap plays a fundamental role in both embryonic and adult neurogenesis.

Despite a normal transcription of Sp1 mRNA in Trrap-deleted cells [48], the Sp1 protein level is greatly reduced in Trrap deficient aNSCs due to proteasomal degradation. As shown before, both acetylation and ubiquitination can modify the same residue K19 on Sp1 [58] while SUMOylation at K16 facilitates proteasomal degradation of Sp1 [52]. Thus, it is plausible that Trrap maintains the acetylation pattern on certain lysine residues, which then competes against ubiquitination/SUMOylation thereby preventing Sp1 from ubiquitin-mediated proteasomal degradation [59]. We find that the acetylation pattern of the documented lysine residues K16, K19, K703 and K639 cannot confer a normal protein level of Sp1 in Trrap deficient aNSCs. These results suggest that Trrap scaffold is essential for its stability, or that other to-be-discovered residues modified by Trrap-HAT stabilizes Sp1.

The deacetylation at K639 and K703 increases Sp1 activity in Trrap mutant cells, suggesting that acetylation at these two sites is inhibitory for Sp1 activity. This seems to be achieved by K639R and K703R mutations that improve the Sp1 binding at promoters of its targets (e.g., p21 and STMN3). In this regard, it worth mentioning that TIP60 acetylates Sp1 at K639 that impairs its promoter binding on target genes, thereby repressing Sp1 activity [57]. In contrast to a previous study that Sp1 deacetylation leads to higher interaction with p300 [56], Sp1 deacetylation mutants (K639R and K703R) compromises Sp1-Trrap interaction, reversely correlating with their Sp1 activity. While p300 and Trrap (or its related HAT) may compete for Sp1 interaction, deacetylated Sp1 (K639R and K703R) antagonizes Trrap binding at gene promoters, which may nevertheless facilitate the recruitment of Trrap-independent HATs for acetylation of histones at promoter regions. In supporting these hypotheses, previous work showed that deacetylated Sp1 recruits p300 to chromatin to acetylate histones

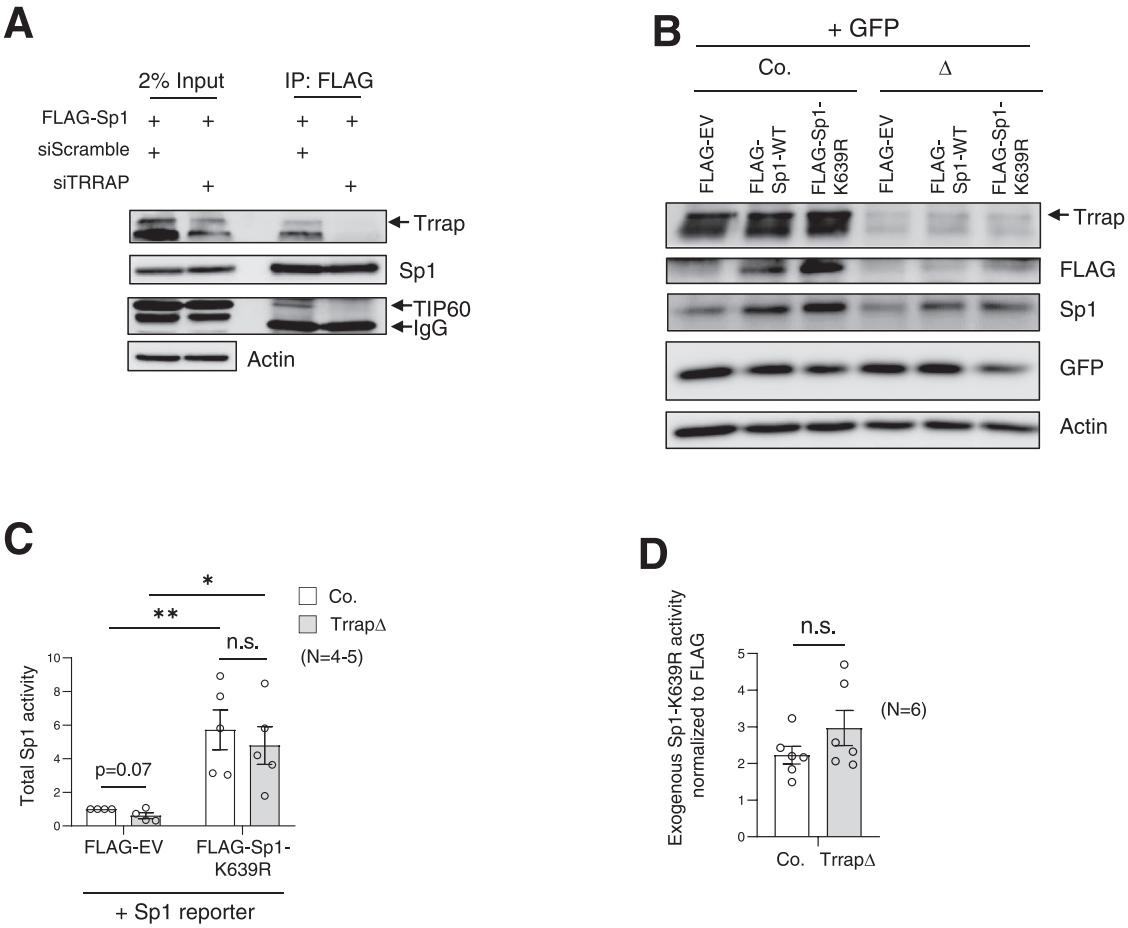

Fig. 6. K639 deacetylation reverses Sp1 activity deficiency after Trrap-deletion, A. Co-IP analysis reveals the interaction between Sp1 and TIP60 in N2A cells. N2A cells were transfected with siRNA against Trrap, followed by 24 hr incubation and FLAG-Sp1 transfection. After another 24 hr incubation, the cells were subjected to co-IP and immunoblotting subsequently. Trrap knockdown abolished the interaction between Sp1 and TIP60. Actin blot acts as a loading control. B. Immunoblot shows the level of exogenous Sp1 variants and total Sp1 in both control and mutant aNSCs co-transfected with FLAG-Sp1, FLAG-Sp1-K639R variants together with GFP. Actin serves a loading control. C. The total Sp1 activity from control and mutant aNSC transfected with the indicated constructs together with Sp1-reporter. Cells from 4 to 5 Trrap$^{f/+}$ and Trrap-aNSCΔ mice analyzed. D. The Sp1 activity is calculated as described in Fig. 4D. Cells from 6 Trrap$^{f/+}$ and 6 Trrap-aNSCΔ mice were analyzed. Mean ± standard error of mean is shown. Paired t-test was performed for statistical analysis in (C-D). n.s.: not significant. *: $p \leq 0.05$, **: $p \leq 0.01$.

around promoter regions thereby promoting transcription [56,70,71]. In addition, acetylation of different lysine residues is catalyzed by specific HATs and have different functional outcomes. For examples, K120 on p53 is acetylated by MOF, which facilitates the acetylation of histones on promoter region and activates the expression of pro-apoptotic genes PUMA and BAX [72]. On the other hand, acetylation of K382 on p53 promotes recruitment of p300 to p21 promoter, leading to increased histone acetylation on the promoter region and subsequently p21 transcription [73]. Thus, the acetylation status of lysine residues of transcription factors may modulate the selective recruitment of specific HATs to the promoters of the target genes.

Despite both deacetylation mutants Sp1-K639R and Sp1-K703R increase Sp1 activity and binding to target gene promoters, only the K639R mutant renders Sp1 resistance to Trrap-deletion-mediated downregulation of Sp1 activity. Since TIP60-mediated acetylation of Sp1 at K639 is inhibitory for its promoter binding [57], in the absence of Trrap (presumably interrupting TIP60), this site could be acetylated by Trrap-independent HATs, which represses Sp1's promoter binding and activity as observed previously [48]. Thus, an ectopic expression of Sp1-K639R forces Sp1 binding, which overcomes the compromised Sp1 promoter binding incurred by other HATs and thereby effectively corrects the differentiation defect of Trrap mutant aNSCs. Therefore, acetylation on K639 is an important regulatory event for Sp1 to grant a full aNSC differentiation capacity in adult neurogenesis.

In the current study, we identify the specific lysine 639 of Sp1 to be a key modification site for Trrap-HAT mediated transcription. The deacetylation at specific K639 on Sp1 facilitates Sp1 binding to chromatin at target promoters, which is normally inhibited by the occupancy of Trrap, thus leading to hyperacetylation of the promoter region for gene transcription (as a readout of Sp1 activity). When Trrap is deleted, K639 on Sp1 is acetylated by Trrap-independent HATs, abolishing the Sp1-chromatin binding and repressing expression of Sp1 targets responsible for adult neurogenesis. Nevertheless, Trrap deletion destabilizes Sp1 and thereby impairs its transcriptional activity, which are possibly due to the deacetylation of other to-be-discovered residues modified by Trrap-HAT, or the lack of Trrap itself, whose scaffold function is necessary for Sp1 stability. These hypotheses are consistent with the notion that TRRAP as scaffold mediates the binding of transcription factors onto target promoter [36,38,43,48,74]. Taken together, we show that a

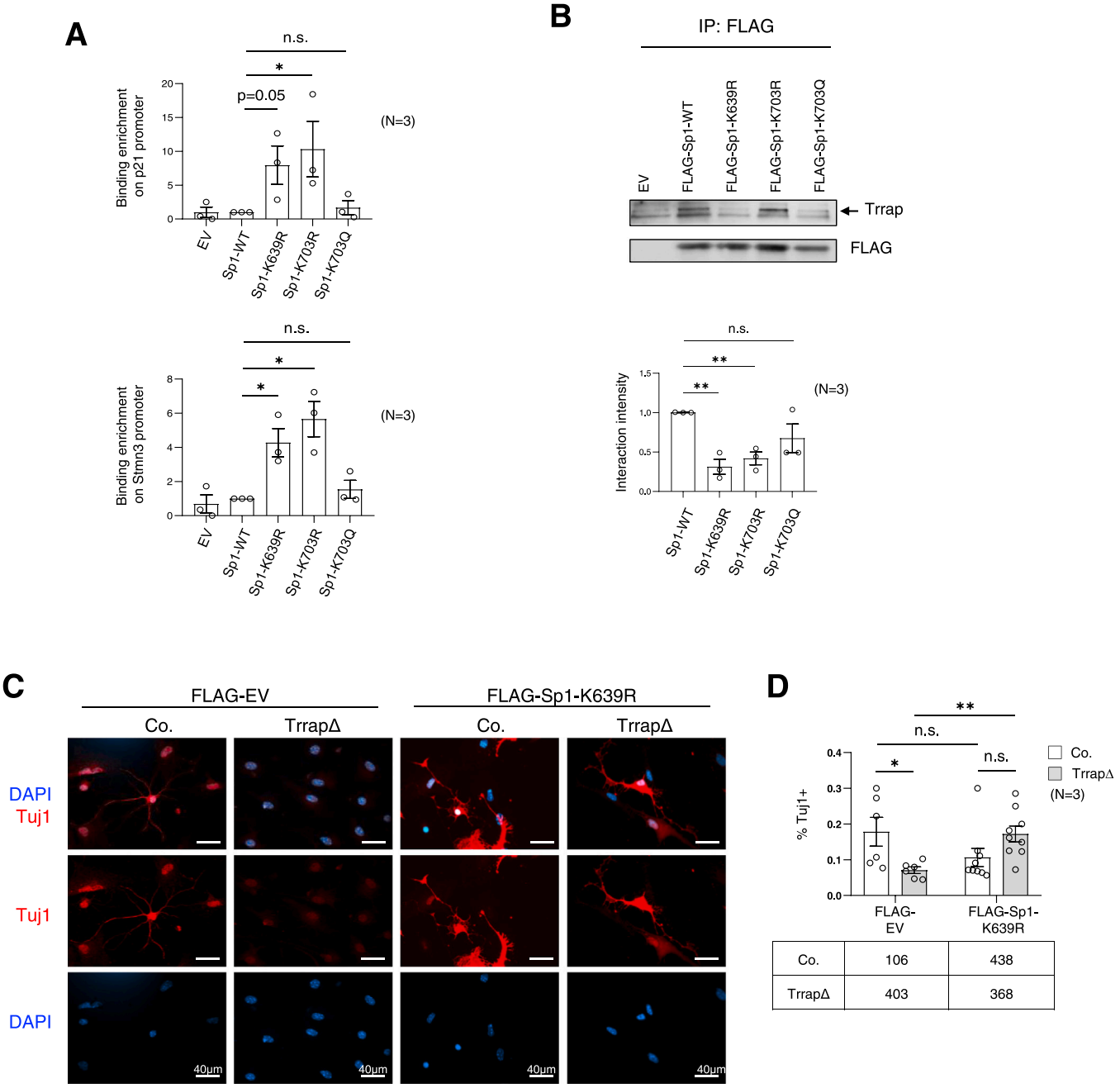

Co.	106	438
TrrapΔ	403	368

Fig. 7. Deacetylation at K639 increases Sp1-promoter binding and rescues the differentiation defect of TrrapΔ-aNSCs, A. ChIP analysis on the promoter of p21 and Stmn3 in N2A cells transfected with FLAG-EV, FLAG-Sp1 or FLAG-Sp1 variants using anti-FLAG antibodies. qPCR analysis was performed to quantify the binding of respective Sp1 variant on target gene promoters. The binding enrichment is presented as fold enrichment over FLAG-Sp1 binding value. The binding value of FLAG-EV, FLAG-Sp1 and FLAG-Sp1 variants was calculated in percentage of input subtracted with IgG binding value in percentage of input. N = 3. B. Co-IP analysis determines the interaction between exogenous Sp1 variants and endogenous Trrap in N2A cells. The interaction strength (right panel) was calculated by dividing the signal intensity of Trrap by the intensity of FLAG in left panel. N = 3. C. Immunofluorescent images showing aNSCs after transfection with FLAG-EV or FLAG-Sp1-K639R at 5 DPD. Cell mixture was stained against neuronal marker Tuj1 (red) and co-stained with DAPI (cyan). Scale bar: 40 μm. D. Quantification of $Tuj1^+$ cells in percentage to total cell population ($DAPI^+$). Cells from 3 $Trrap^{f/+}$ and Trrap-aNSCΔ mice analyzed. Mean ± standard error of mean is shown. Paired t-test was performed for statistical analysis in (A-B). Unpaired t-test was performed for statistical analysis in (D). n.s.: not significant. *: $p \leq 0.05$, **: $p \leq 0.01$.

fine-tuning of Sp1 activity via Trrap-HAT is critical for controlling the cell fate of aNSCs during adult neurogenesis.

CRediT authorship contribution statement

B.-K. Y., conceived the project, performed the majority of the experiments, interpreted the data and wrote the manuscript. D.L. executed the in vivo study of Trrap-aNSCΔ mice. Z.-Q.W. designed the experiments, supervised the project and wrote the manuscript.

Conflict of interest

There is no competing interests.

Acknowledgments

We thank P. Grigaravicius for his advice and discussion. We also thank P. Elsner for his excellent assistance in the maintenance of the animal colonies. We are grateful to the FLI Core Facilities Histology

and Imaging for their technical support. We thank members of Wang Laboratory for their helpful and critical discussions. B.-K.Y. was a Ph.D. candidate from the Leibniz Graduate School on Aging (LGSA). D.L. was a recipient of Ph.D. studentship from the LGSA. Wang Laboratory is supported by the Leibniz Association, Germany.

Author statement

All *authors* have seen and approved the final version of the manuscript being submitted. They warrant that the article is the *authors*' original work, hasn't received prior publication and isn't under consideration for publication elsewhere.

Appendix A. Supporting information

Supplementary data associated with this article can be found in the online version at doi:10.1016/j.csbj.2022.12.024.

References

[1] Verma V, Paul A, Amrapali Vishwanath A, Vaidya B, Clement JP. Understanding intellectual disability and autism spectrum disorders from common mouse models: synapses to behaviour. Open Biol 2019;9:180265.
[2] Chiurazzi P, et al. Genetic analysis of intellectual disability and autism. Acta Biomed 2020;91:e2020003.
[3] Fares J, Bou Diab Z, Nabha S, Fares Y. Neurogenesis in the adult hippocampus: history, regulation, and prospective roles. Int J Neurosci 2019;129:598–611.
[4] Ming GL, Song H. Adult neurogenesis in the mammalian central nervous system. Annu Rev Neurosci 2005;28:223–50.
[5] Batailler M, et al. DCX-expressing cells in the vicinity of the hypothalamic neurogenic niche: a comparative study between mouse, sheep, and human tissues. J Comp Neurol 2014;522:1966–85.
[6] Giap BT, Jong CN, Ricker JH, Cullen NK, Zafonte RD. The hippocampus: anatomy, pathophysiology, and regenerative capacity. J Head Trauma Rehabil 2000;15:875–94.
[7] Pak S, et al. Hippocampal interlamellar cell-cell connectome that counts. J Cell Physiol 2022.
[8] Gu Y, Janoschka S, Ge S. Neurogenesis and hippocampal plasticity in adult brain. Curr Top Behav Neurosci 2013;15:31–48.
[9] Chen P, Chen F, Wu Y, Zhou B. New insights into the role of aberrant hippocampal neurogenesis in epilepsy. Front Neurol 2021;12:727065.
[10] Blankers SA, Galea LAM. Androgens and adult neurogenesis in the hippocampus. Androg Clin Res Ther 2021;2:203–15.
[11] Hernandez-Mercado K, Zepeda A. Morris water maze and contextual fear conditioning tasks to evaluate cognitive functions associated with adult hippocampal neurogenesis. Front Neurosci 2021;15:782947.
[12] Li Y, Guo W. Neural stem cell niche and adult neurogenesis. Neuroscientist 2021;27:235–45.
[13] Audesse AJ, Webb AE. Mechanisms of enhanced quiescence in neural stem cell aging. Mech Ageing Dev 2020;191:111323.
[14] Tassinari M, et al. Luteolin treatment ameliorates brain development and behavioral performance in a mouse model of CDKL5 deficiency disorder. Int J Mol Sci 2022;23.
[15] Javadi S, et al. Sustained correction of hippocampal neurogenic and cognitive deficits after a brief treatment by Nutlin-3 in a mouse model of fragile X syndrome. BMC Med 2022;20:163.
[16] Okano H, et al. Ameliorating effect of continuous alpha-glycosyl isoquercitrin treatment starting from late gestation in a rat autism model induced by postnatal injection of lipopolysaccharides. Chem Biol Interact 2022;351 :109767.
[17] Kotagiri P, Chance SA, Szele FG, Esiri MM. Subventricular zone cytoarchitecture changes in autism. Dev Neurobiol 2014;74:25–41.
[18] Hoeft F, et al. Morphometric spatial patterns differentiating boys with fragile X syndrome, typically developing boys, and developmentally delayed boys aged 1 to 3 years. Arch Gen Psychiatry 2008;65:1087–97.
[19] Hazlett HC, et al. Teasing apart the heterogeneity of autism: Same behavior, different brains in toddlers with fragile X syndrome and autism. J Neurodev Disord 2009;1:81–90.
[20] de von Flindt R, Bybel B, Chudley AE, Lopes F. Short-term memory and cognitive variability in adult fragile X females. Am J Med Genet 1991;38:488–92.
[21] Greicius MD, Boyett-Anderson JM, Menon V, Reiss AL. Reduced basal forebrain and hippocampal activation during memory encoding in girls with fragile X syndrome. Neuroreport 2004;15:1579–83.
[22] Li Y, et al. MDM2 inhibition rescues neurogenic and cognitive deficits in a mouse model of fragile X syndrome. Sci Transl Med 2016;8. (336ra361).
[23] Pinar C, et al. Effects of voluntary exercise on cell proliferation and neurogenesis in the dentate gyrus of adult FMR1 knockout mice. Brain Plast 2018;4:185–95.
[24] Lazarov O, et al. Impaired survival of neural progenitor cells in dentate gyrus of adult mice lacking fMRP. Hippocampus 2012;22:1220–4.
[25] Stagni F, et al. Neonatal treatment with cyclosporine A restores neurogenesis and spinogenesis in the Ts65Dn model of Down syndrome. Neurobiol Dis 2019;129:44–55.
[26] Zou D, et al. A critical role of RBM8a in proliferation and differentiation of embryonic neural progenitors. Neural Dev 2015;10:18.
[27] Grasselli C, et al. Neural stem cells from shank3-ko mouse model autism spectrum disorders. Mol Neurobiol 2020;57:1502–15.
[28] Tapias A, Wang ZQ. Lysine acetylation and deacetylation in brain development and neuropathies. Genom Proteom Bioinform 2017;15:19–36.
[29] Levenson JM, Sweatt JD. Epigenetic mechanisms in memory formation. Nat Rev Neurosci 2005;6:108–18.
[30] Delgado-Morales R, Agis-Balboa RC, Esteller M, Berdasco M. Epigenetic mechanisms during ageing and neurogenesis as novel therapeutic avenues in human brain disorders. Clin Epigenet 2017;9:67.
[31] Berson A, Nativio R, Berger SL, Bonini NM. Epigenetic regulation in neurodegenerative diseases. Trends Neurosci 2018;41:587–98.
[32] Valor LM. Understanding histone deacetylation in Huntington's disease. Oncotarget 2017;8:5660–1.
[33] Park G, et al. Regulation of histone acetylation by autophagy in Parkinson Disease. J Biol Chem 2016;291:3531–40.
[34] Klein HU, et al. Epigenome-wide study uncovers large-scale changes in histone acetylation driven by tau pathology in aging and Alzheimer's human brains. Nat Neurosci 2019;22:37–46.
[35] Yin BK, Wang ZQ. Beyond HAT adaptor: TRRAP Liaisons with Sp1-mediated transcription. Int J Mol Sci 2021;22.
[36] Li H, Cuenin C, Murr R, Wang ZQ, Herceg Z. HAT cofactor Trrap regulates the mitotic checkpoint by modulation of Mad1 and Mad2 expression. EMBO J 2004;23:4824–34.
[37] Kwan SY, et al. Depletion of TRRAP induces p53-independent senescence in liver cancer by down-regulating mitotic genes. Hepatology 2020;71:275–90.
[38] DeRan M, Pulvino M, Greene E, Su C, Zhao J. Transcriptional activation of histone genes requires NPAT-dependent recruitment of TRRAP-Tip60 complex to histone promoters during the G1/S phase transition. Mol Cell Biol 2008;28:435–47.
[39] Struhl K. Histone acetylation and transcriptional regulatory mechanisms. Genes Dev 1998;12:599–606.
[40] Murr R, Vaissiere T, Sawan C, Shukla V, Herceg Z. Orchestration of chromatin-based processes: mind the TRRAP. Oncogene 2007;26:5358–72.
[41] Kang KT, et al. TRRAP stimulates the tumorigenic potential of ovarian cancer stem cells. BMB Rep 2018;51:514–9.
[42] Loizou JI, et al. Histone acetyltransferase cofactor Trrap is essential for maintaining the hematopoietic stem/progenitor cell pool. J Immunol 2009;183:6422–31.
[43] Tapias A, et al. Trrap-dependent histone acetylation specifically regulates cell-cycle gene transcription to control neural progenitor fate decisions. Cell Stem Cell 2014;14:632–43.
[44] Herceg Z, et al. Disruption of Trrap causes early embryonic lethality and defects in cell cycle progression. Nat Genet 2001;29:206–11.
[45] Xia W, et al. Novel TRRAP mutation causes autosomal dominant non-syndromic hearing loss. Clin Genet 2019;96:300–8.
[46] Cogne B, et al. Missense variants in the histone acetyltransferase complex component gene TRRAP cause autism and syndromic intellectual disability. Am J Hum Genet 2019;104:530–41.
[47] Mavros CF, et al. De novo variant of TRRAP in a patient with very early onset psychosis in the context of non-verbal learning disability and obsessive-compulsive disorder: a case report. BMC Med Genet 2018;19:197.
[48] Tapias A, et al. HAT cofactor TRRAP modulates microtubule dynamics via SP1 signaling to prevent neurodegeneration. eLife 2021;10.
[49] O'Connor L, Gilmour J, Bonifer C. The role of the ubiquitously expressed transcription factor Sp1 in tissue-specific transcriptional regulation and in disease. Yale J Biol Med 2016;89:513–25.
[50] Samson SL, Wong NC. Role of Sp1 in insulin regulation of gene expression. J Mol Endocrinol 2002;29:265–79.
[51] Suzuki T, Kimura A, Nagai R, Horikoshi M. Regulation of interaction of the acetyltransferase region of p300 and the DNA-binding domain of Sp1 on and through DNA binding. Genes Cells 2000;5:29–41.
[52] Wang YT, Yang WB, Chang WC, Hung JJ. Interplay of posttranslational modifications in Sp1 mediates Sp1 stability during cell cycle progression. J Mol Biol 2011;414:1–14.
[53] Spengler ML, Guo LW, Brattain MG. Phosphorylation mediates Sp1 coupled activities of proteolytic processing, desumoylation and degradation. Cell Cycle 2008;7:623–30.
[54] Kang-Park S, Lee JH, Shin JH, Lee YI. Activation of the IGF-II gene by HBV-X protein requires PKC and p44/p42 map kinase signalings. Biochem Biophys Res Commun 2001;283:303–7.
[55] Cieslik K, Abrams CS, Wu KK. Up-regulation of endothelial nitric-oxide synthase promoter by the phosphatidylinositol 3-kinase gamma /Janus kinase 2/MEK-1-dependent pathway. J Biol Chem 2001;276:1211–9.
[56] Hung JJ, Wang YT, Chang WC. Sp1 deacetylation induced by phorbol ester recruits p300 to activate 12(S)-lipoxygenase gene transcription. Mol Cell Biol 2006;26:1770–85.
[57] Rajagopalan D, et al. TIP60 represses telomerase expression by inhibiting Sp1 binding to the TERT promoter. PLOS Pathog 2017;13:e1006681.
[58] Elia AE, et al. Quantitative proteomic atlas of ubiquitination and acetylation in the DNA damage response. Mol Cell 2015;59:867–81.
[59] Li M, Luo J, Brooks CL, Gu W. Acetylation of p53 inhibits its ubiquitination by Mdm2. J Biol Chem 2002;277:50607–11.

[60] Zhu G, et al. Pten deletion causes mTorc1-dependent ectopic neuroblast differentiation without causing uniform migration defects. Development 2012;139:3422–31.
[61] Ventura A, et al. Restoration of p53 function leads to tumour regression in vivo. Nature 2007;445:661–5.
[62] Courey AJ, Tjian R. Analysis of Sp1 in vivo reveals multiple transcriptional domains, including a novel glutamine-rich activation motif. Cell 1988;55:887–98.
[63] Muzumdar MD, Tasic B, Miyamichi K, Li L, Luo L. A global double-fluorescent Cre reporter mouse. Genesis 2007;45:593–605.
[64] Guerra GM, et al. Cell type-specific role of RNA nuclease SMG6 in neurogenesis. Cells 2021;10.
[65] Pascal E, Tjian R. Different activation domains of Sp1 govern formation of multimers and mediate transcriptional synergism. Genes Dev 1991;5:1646–56.
[66] Karkhanis M, Park JI. Sp1 regulates Raf/MEK/ERK-induced p21(CIP1) transcription in TP53-mutated cancer cells. Cell Signal 2015;27:479–86.
[67] Hirabayashi Y, Gotoh Y. Epigenetic control of neural precursor cell fate during development. Nat Rev Neurosci 2010;11:377–88.
[68] Tsankova N, Renthal W, Kumar A, Nestler EJ. Epigenetic regulation in psychiatric disorders. Nat Rev Neurosci 2007;8:355–67.
[69] Encinas JM, et al. Division-coupled astrocytic differentiation and age-related depletion of neural stem cells in the adult hippocampus. Cell Stem Cell 2011;8:566–79.
[70] Hepp MI, et al. A Trichostatin A (TSA)/Sp1-mediated mechanism for the regulation of SALL2 tumor suppressor in Jurkat T cells. Biochim Biophys Acta Gene Regul Mech 2018.
[71] Li G, et al. Sp1-mediated epigenetic dysregulation dictates HDAC inhibitor susceptibility of HER2-overexpressing breast cancer. Int J Cancer 2019;145:3285–98.
[72] Li X, Wu L, Corsa CA, Kunkel S, Dou Y. Two mammalian MOF complexes regulate transcription activation by distinct mechanisms. Mol Cell 2009;36:290–301.
[73] Barlev NA, et al. Acetylation of p53 activates transcription through recruitment of coactivators/histone acetyltransferases. Mol Cell 2001;8:1243–54.
[74] Unno A, et al. TRRAP as a hepatic coactivator of LXR and FXR function. Biochem Biophys Res Commun 2005;327:933–8.